

Article

Characteristics of Mineralogy, Lithofacies of Fine-Grained Sediments and Their Relationship with Sedimentary Environment: Example from the Upper Permian Longtan Formation in the Sichuan Basin

Hongzhi Yang¹, Liangbiao Lin^{2,3,*}, Liqing Chen¹, Yu Yu², Du Li¹, Jingchun Tian³, Wen Zhou^{2,4}  and Jianhua He^{2,4}

¹ PetroChina Southwest Oil & Gasfield Company, Chengdu 610051, China; yanghz@petrochina.com.cn (H.Y.); chenlq28@petrochina.com.cn (L.C.); du@petrochina.com.cn (D.L.)

² State Key Laboratory of Oil and Gas Reservoir Geology and Exploitation, Chengdu University of Technology, Chengdu 610059, China; yuyu@cdut.edu.cn (Y.Y.); zhouw62@cdut.edu.cn (W.Z.); hejianhua19@cdut.edu.cn (J.H.)

³ Institute of Sedimentary Geology, Chengdu University of Technology, Chengdu 610059, China; tjc@cdut.edu.cn

⁴ College of Energy, Chengdu University of Technology, Chengdu 610059, China

* Correspondence: linliangbiao08@cdut.cn



Citation: Yang, H.; Lin, L.; Chen, L.; Yu, Y.; Li, D.; Tian, J.; Zhou, W.; He, J. Characteristics of Mineralogy, Lithofacies of Fine-Grained Sediments and Their Relationship with Sedimentary Environment: Example from the Upper Permian Longtan Formation in the Sichuan Basin. *Energies* **2021**, *14*, 3662. <https://doi.org/10.3390/en14123662>

Academic Editor: Reza Rezaee

Received: 11 May 2021

Accepted: 17 June 2021

Published: 19 June 2021

Publisher's Note: MDPI stays neutral with regard to jurisdictional claims in published maps and institutional affiliations.



Copyright: © 2021 by the authors. Licensee MDPI, Basel, Switzerland. This article is an open access article distributed under the terms and conditions of the Creative Commons Attribution (CC BY) license (<https://creativecommons.org/licenses/by/4.0/>).

Abstract: The Longtan Formation of the Upper Permian in the Sichuan Basin has become a significant target for shale gas exploration in recent years. Multiple methods, including outcrop observations, thin sections, total organic matter content, X-ray diffraction and scanning electron microscopy were used to investigate the mineralogy, shale lithofacies assemblages and their relationships with the deposition environment. The mineral composition of the Longtan Formation has strong mineral heterogeneity. The TOC values of the Longtan Formation have a wide distribution range from 0.07% to 74.67% with an average value of 5.73%. Four types of shale lithofacies assemblages of the Longtan Formation could be distinguished, as clayey mudstone (CLS), carbonaceous shale (CAS), siliceous shale (SS) and mixed shale (MS) on the basis of mineral compositions. The TOC values of various types of shale lithofacies assemblages in the Longtan Formation varied widely. The shore swamp of the Longtan Formation is most influenced by the terrestrial input and mainly develops CLS and MS. The tidal flat is influenced by the terrestrial input and can also deposit carbonate minerals, developing CLS, CAS and MS. The shallow water melanged accumulation shelf develops CAS and MS, dominated by clay and carbonate minerals. The deep water miscible shelf develops CLS and SS, whose mineral composition is similar to that of the shore swamp, but the quartz minerals are mainly formed by chemical and biological reactions, which are related to the Permian global chert event. The depositional environment of the Longtan Formation controls the shale mineral assemblage of the Longtan Formation and also influences the TOC content.

Keywords: TOC; shale lithofacies assemblages; deposition environment; the Late Permian; Sichuan Basin

1. Introduction

In the past few years, huge breakthroughs have been undertaken in shale gas exploration in Sichuan Basin [1–6]. Following the Niutitang Formation and Wufeng-Longmaxi Formation, another set of Paleozoic mudstone in the Sichuan Basin, the Longtan Formation, has attracted more and more attention [4,7–9]. Previous scholars have studied the geochemical characteristics and evaluated the potential of shale gas of the Longtan shale, and the results show enormous potential and exploration prospects [2,4,10–14].

Fine-grained sediments refer to sediment with a grain size of less than 0.062 mm [15] and are the main constituents (the content of grain less than 0.062 mm is more than 50%) of

mudstone and shale. The sedimentary environment exerts serious control on the distribution and characteristics of sediments [16], making the study of lithofacies and sedimentary environment crucial for fine-grained sediments [16–19]. Frequent volcanic activity took place in the Yangtze region in the Permian, and the ‘Emeishan basalt’ erupted at the turn of the Middle and Late Permian, which seriously changed the paleogeographic pattern of the Upper Yangtze region [4,20–22]. Then, during the Late Permian, fine-grained sediments of the Longtan Formation deposited under the marine-terrestrial environment occurred in the eastern of the Sichuan Basin [20], however, complex mineral and lithologic compositions make the shale highly heterogeneous, which seriously impedes shale exploration. The mineralogical and lithofacies characteristics of the Longtan Formation shale and their relationship with the sedimentary environment are studied in detail. These studies are beneficial to the exploration of shale gas in the area and provide a basis for restoring the paleoenvironment of the Upper Yangtze region in the Late Permian.

The aim of this paper is to present data on mineralogy, total organic carbon (TOC), lithofacies and their relationships with sedimentary environment of the Longtan Formation. Descriptions of geological setting and distribution of sedimentary facies of the Longtan Formation in the eastern Sichuan Basin are based on previous studies [4,23]. The petrology, mineralogy and lithofacies of the Longtan shale were studied by multiple methods, including outcrop observations, thin-section, TOC, X-ray diffraction (XRD) and scanning electron microscopy (SEM).

2. Geological Setting and Sedimentary Facies of Longtan Formation

The Sichuan Basin that is one of most important petroliferous basins in China (Figure 1A). The Sichuan Basin is located in the Upper Yangtze region, bordered by Longmenshan thrust belt in the west and joined by the Songpan-Ganzi tectonic belt [20,24]. Sichuan Basin is a multi-cycle sedimentary basin with strata over 10 km from the Sinian to the Quaternary, in which marine deposits dominated from the Sinian to Middle Triassic, and mainly continental lacustrine basin deposits from the Upper Triassic to Quaternary [25].

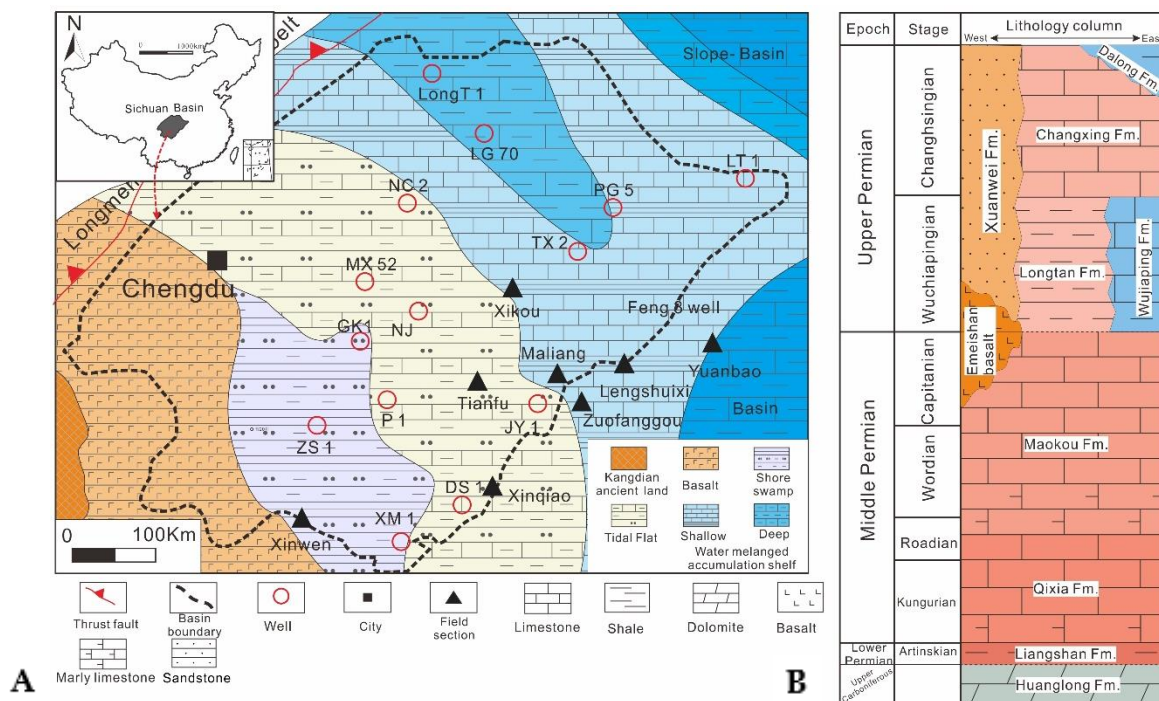


Figure 1. (A) The geological setting and the paleogeographic maps of the Longtan Formation of the Sichuan Basin; (B) Simplified stratigraphic column of the Permian in the Sichuan Basin.

The crystalline basement of the Sichuan Basin formed 800 Ma ago, followed by several major tectonic movements: Jinning, Caledonian, Yunnan, Hercynian (Dongwu), Indosinian, Yanshanian, and Himalayan movements [25,26]. Under the influence of Caledonian and Yunnan movements, the Sichuan Basin continued to uplift. Apart from the Carboniferous Huanglong Formation that occurred in the east of the basin and the Lower Permian Liangshan Formation, Devonian, Carboniferous and Lower Permian were extensively absent in the basin. The Dongwu movement between Middle and Late Permian was accompanied by large-scale basalt eruption in the southwest of the basin, i.e., Emeishan basalt, which is a large igneous province (LIP) related to the rise of mantle plume [27]. Affected by this, the sedimentary differentiation pattern of the Late Permian Sichuan Basin is distinct. From the southwestern margin of the basin, continental, transitional and marine environments are distributed in turn (Figure 1B): Xuanwei Formation is dominated by terrestrial siliciclastic rocks developed in the southwestern margin of the basin; Longtan Formation deposited in a transitional environment consists of fine-grained sediments, such as mudstone, shale, siltstone and coal seam, distributed in the center and east of the basin; Wujiaping Formation with a set of carbonate sediments deposited in a marine environment in the north and east of the basin [20]. Among them, the deposition time of the Xuanwei Formation spanned the entire Late Permian, while for the Longtan and Wujiaping Formation took place during the Wuchiapingian, upward to the Changhsingian, lithostratigraphic units became Changxing Formation and Dalong Formation (Figure 1B).

This paper focused on the fine-grained sediments of the Wuchiapingian of the Sichuan Basin, i.e., Longtan Formation and Wujiaping Formation (Figure 1). Based on the previous studies, the paleogeographic maps of the Longtan Formation in the Sichuan Basin show that sedimentary facies can be divided into fluvial, shore, tidal flat, melanged accumulation shelf and platform basin from the southwest to northeast of the basin (Figure 1A). Frequent sedimentary facies changes resulted in obvious lateral changes in lithologic of the Longtan Formation. The lithology of Longtan Formation is grey-black shale and mudstone with siltstone, thin layer sandstone and coal seam; the bottom lithology of Wujiaping Formation is carbonaceous shale and aluminous mudstone, with an upward transition to dark gray limestone with mudstone and chert (Figure 1B). In order to facilitate the expression, the two are collectively referred to as the Longtan Formation.

3. Material and Methods

In this paper, the Longtan shale samples were collected from six wells (LG70, LongT1, NC2, LT1, DS1 and MX52) and eight field outcrops, as show in Figure 2. Field outcrops observation was mainly used to study the sedimentary structure, macroscopic lithofacies and petrological characteristics of the Longtan Formation. In this paper, analytical multi-techniques, including thin sections, XRD ($n = 14$), TOC ($n = 114$) and SEM ($n = 20$) were used to obtain microscopic petrological and mineralogy characteristics from samples selected from outcrops and wells.

A Leica polarizing microscope was used to observe thin sections stained with Alizatin Red S dye. SEM was performed by a Quanta250 FEG with Oxford INCAx-max20 energy dispersive spectrometer (EDS) in the State Key Laboratory of Oil and Gas Reservoir Geology and Exploitation (Chengdu University of Technology) to investigate the morphology of minerals and qualitative or semi-quantitative microanalysis.

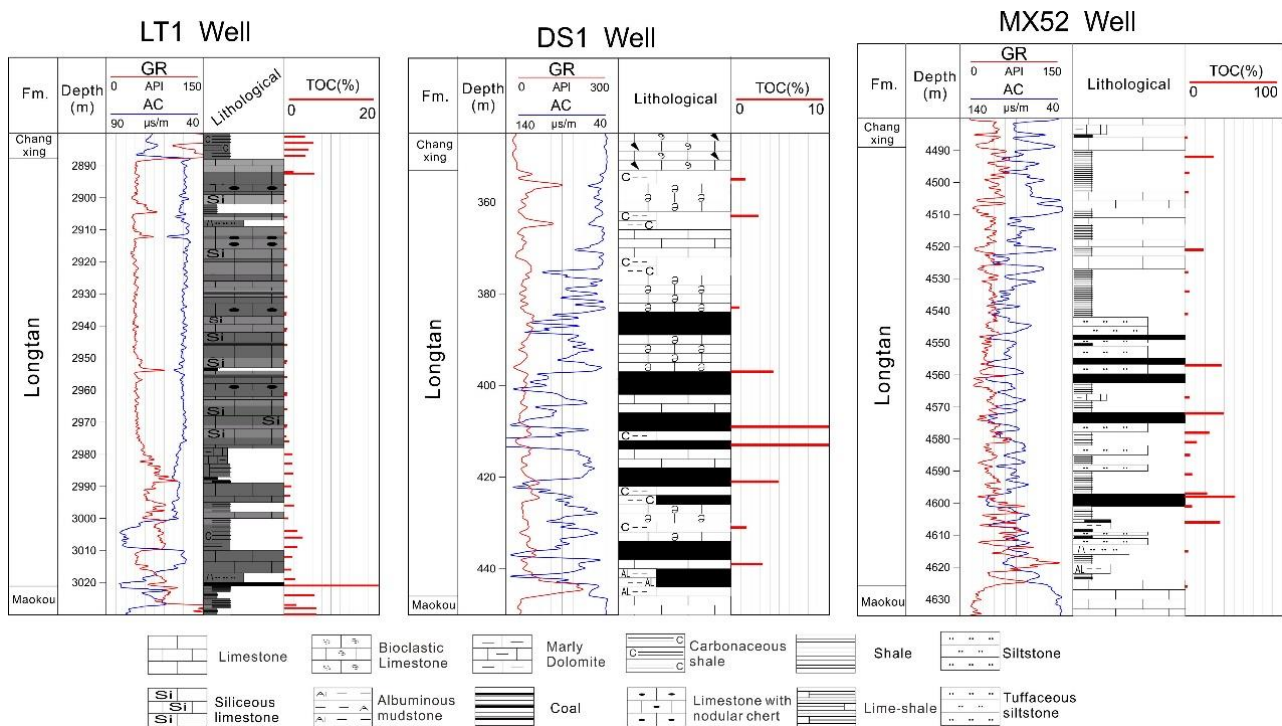


Figure 2. Lithological column and TOC of LT1 well, DS1 well and MX52 well.

XRD was performed using an XRF-1800 for bulk and clay mineralogy, to obtain precise contents of minerals. First, 10 g of samples were crushed to 200 mesh, then, the sample powder was put into the sample mold of the instrument and compacted uniformly by the back pressure method, with the downward side used as the test surface. The samples were analyzed at 40 kV, 40 Ma and a scan rate of $2^{\circ}/\text{min}$ over a range of 5° to 65° . TOC values were determined using a Leco CS-400 carbon/sulfur analyzer at Keyuan Engineering Testing Center, Sichuan. Inorganic carbon was removed by hydrochloric acid from samples. After the remaining samples were dried, the decarburized samples were heated to 1200°C under a stream of oxygen to convert organic carbon to carbon dioxide.

4. Results

4.1. Mineralogy

The XRD results show that the composition of the Longtan shale includes quartz, clay minerals, feldspar, carbonate minerals, barite and a small amount of pyrite, gypsum and anatase (Table 1). The XRD results of the Longtan Formation show that the content of quartz ranges from 7.8% to 39% with an average value of 20.3%, clay minerals content ranges from 1.4% to 20.1% with an average value of 10.3%, potash feldspar content ranges from 0 to 0.9% with an average value of 0.2%, plagioclase content ranges from 0 to 11.3% with an average value of 2.5%, calcite content ranges from 3.8% to 59.7% with an average value of 32.2%, dolomite content ranges from 3% to 15% with an average value of 8.4%, pyrite content ranges from 0 to 7.1% with an average value of 2.9%, siderite content ranges from 0 to 30.4% with an average value of 5.5%. The mineral composition of Longtan Formation shows strong heterogeneity (Figure 3).

Table 1. The mineral composition (%) of the Longtan Formation shale in the eastern Sichuan Basin. (In this table, Q. = quartz, PF. = potash feldspar, PL. = plagioclase, Cal. = calcite, Dol. = dolomite, An. = anatase, Ba. = barite, Py. = pyrite, Sid. = siderite).

Well	Depth (m)	Q.	PF.	PL.	Cal.	Dol.	An.	Ba.	Py.	Sid.	Clay
LG70	7090	7.8	0.9	1.0	44.8	12.1	3.6	2.1	2.4	5.5	19.8
LG70	7115	9.9	0.9	/	49.7	9.5	3.9	/	3.1	6.8	16.2
LG70	7128	7.9	0.9	1.0	45.4	9.5	/	3.6	4.8	6.8	20.1
LG70	7152	24.3	0.5	0.9	52.7	5.8	1.1	2.0	3.0	/	9.7
LG70	7156	25.0	/	1.5	39.1	14.4	0.8	2.7	3.6	/	12.9
LongT1	5660	8.1	/	8.1	48.3	15.0	/	3.3	3.1		14.1
LongT1	5696	26.5	/	1.4	52.2	9.1	/	2.4	3.1		5.3
LongT1	5706	19.2	/	0.6	59.7	6.3	/	4.9	3.1		6.2
NC2	5803	26.2	/	11.3	22.4	9.3	/	10.4	0.7	/	3.1
NC2	5828	38.6	/	2.3	5.1	6.6	/	13.0	2.8	11.5	3.4
NC2	5834	39.0	/	2.4	3.8	3.0	/	16.0	4.1	6.3	1.4
NC2	5853	25.8	/	5.1	7.6	6.7	/	7.1	7.1	30.4	10.2
NC2	5879	15.9	/	/	12.1	12.6	/	34.3	/	9.7	15.4
NC2	5897	15.0	/	/	10.0	9.0	/	55.1	/	4.9	6.0

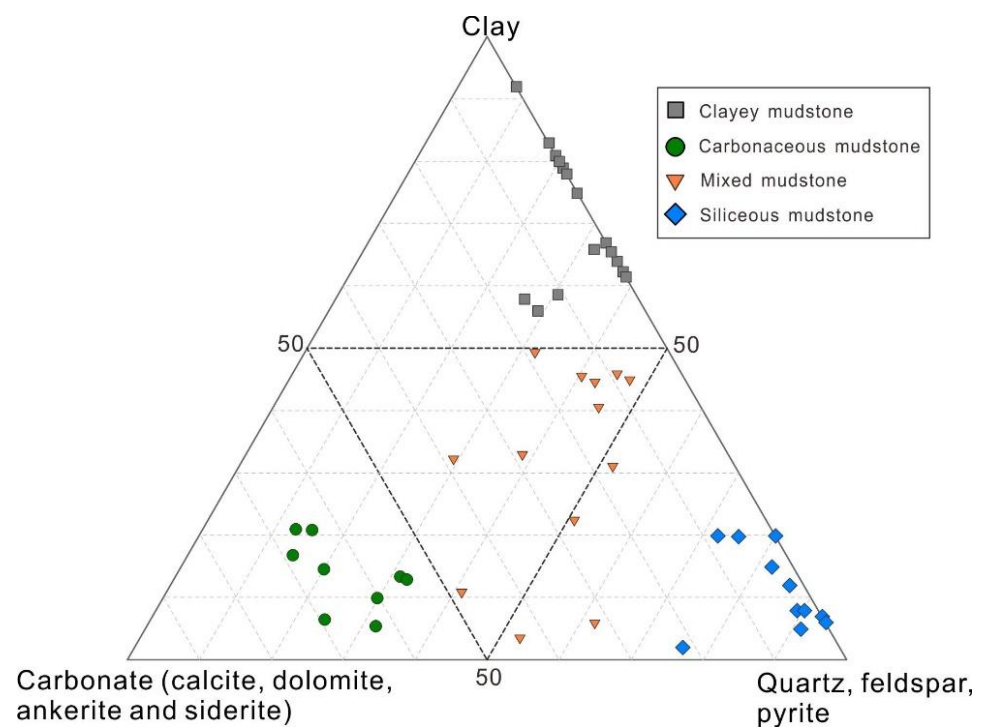


Figure 3. Clay–carbonate–rigid particles (quartz, feldspar and pyrite) minerals ternary diagram and lithofacies types classification of the Longtan Formation.

4.2. Total Organic Carbon

TOC is one of the most significant indices in shale gas exploration, and initial TOC indicates better exploration potential [28,29]. Currently, the lower limit of TOC for the commercial exploitation of shale gas is 2.0 wt.%; however, a few scholars suggested that the lower limit of TOC for shale at the high-maturity stage can be reduced to 1.0 wt.% [1,30,31]. The Longtan Formation deposited under the marine-terrestrial transitional environment and marine environment has complex lithology and huge differences in TOC content. The TOC values of the Longtan Formation ($n = 114$) has a wide distribution range from 0.07 wt.% to 74.67 wt.% with an average value of 5.73 wt.% (median value of 1.59 wt.%), among them, the TOC content of coal is relatively high with a range from 55.1 wt.% to 74.67 wt.% (Figure 4). Although the TOC peak is between 0.5 wt.% and 2 wt.%, the proportion of

mudstone with TOC content greater than 2 wt.% is 63.21%, indicating that the Longtan Formation has huge shale exploration potential.

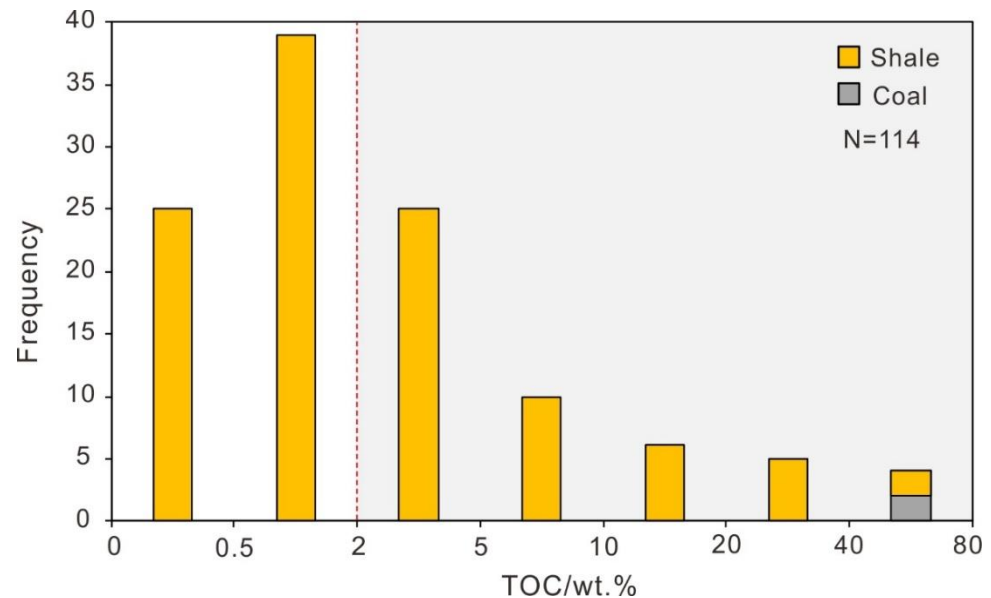


Figure 4. Frequency of distribution histogram of TOC of Longtan Formation mudstone in the Sichuan Basin.

4.3. Shale Lithofacies Assemblages

Considering the complex lithological characteristics of the Longtan Formation, in this paper, the lithofacies of the Longtan shale were divided on the basis of mineral composition [17,32]. Combined with thin sections, SEM, XRD analysis and previous XRD results of the Longtan Formation [4], four types of lithofacies assemblages could be distinguished: clayey mudstone, carbonaceous shale, siliceous shale and mixed shale. XRD results show huge differences among the various lithofacies (Table 2).

Table 2. Mineral compositions and sedimentary facies of the Longtan various shale.

Lithofacies	Mineral Composition (%)			Sedimentary Facies
	Quartz+ Pyrite+ Feldspar	Carbonate	Clay	
Clayey shale	25.13	2.56	66.93	shore swamp; tidal flat; deep water melanged accumulation shelf
Carbonaceous shale	20.42	56.86	12.09	tidal flat; shallow water melanged accumulation shelf
Siliceous shale	81.32	3.65	11.04	deep water melanged accumulation shelf
Mixed shale	38.93	19.98	28.43	shore swamp; tidal flat; shallow water melanged accumulation shelf

4.3.1. Clayey Shale

Clayey shale (CLS) is the predominant lithofacies in the Longtan shale, mainly composed of clay minerals, and other components including quartz, feldspar and carbonate minerals, which generally have high TOC value. The clay minerals content ranges from 51% to 92% with an average value of 66.93%, and the quartz+ pyrite+ feldspar content ranges from 8% to 36% with an average value of 25.13%, carbonate minerals ranges from 0 to 15% with average value of 2.56%. Clayey shale is widely distributed in shore swamp, tidal flat and deep water melanged accumulation shelf. In the shore swamp and tidal flat, the thickness of a single layer of clayey shale is about 0.2~0.8m (Figure 5A) and interspersed

with muddy or calcareous nodules (Figure 5B), interbedded with thin layered coal seams, siltstone and argillaceous siltstone of less than 10 cm (Figure 5B). Horizontal bedding reflecting that the clayey shale deposited under a low-energy environment. Besides, plant fossil fragments could be observed in the thin sections and SEM images (Figure 5C,D). In the deep water melanged accumulation shelf, clayey shale has higher quartz content and lower clay minerals content with parallel bedding (Figure 5E,F). Ammonites with a length of 2~4 cm suggesting a deep water environment (Figure 5E,F), black organic matter and clay minerals occurring in parallel laminar could be observed in SEM images (Figure 5G,H).

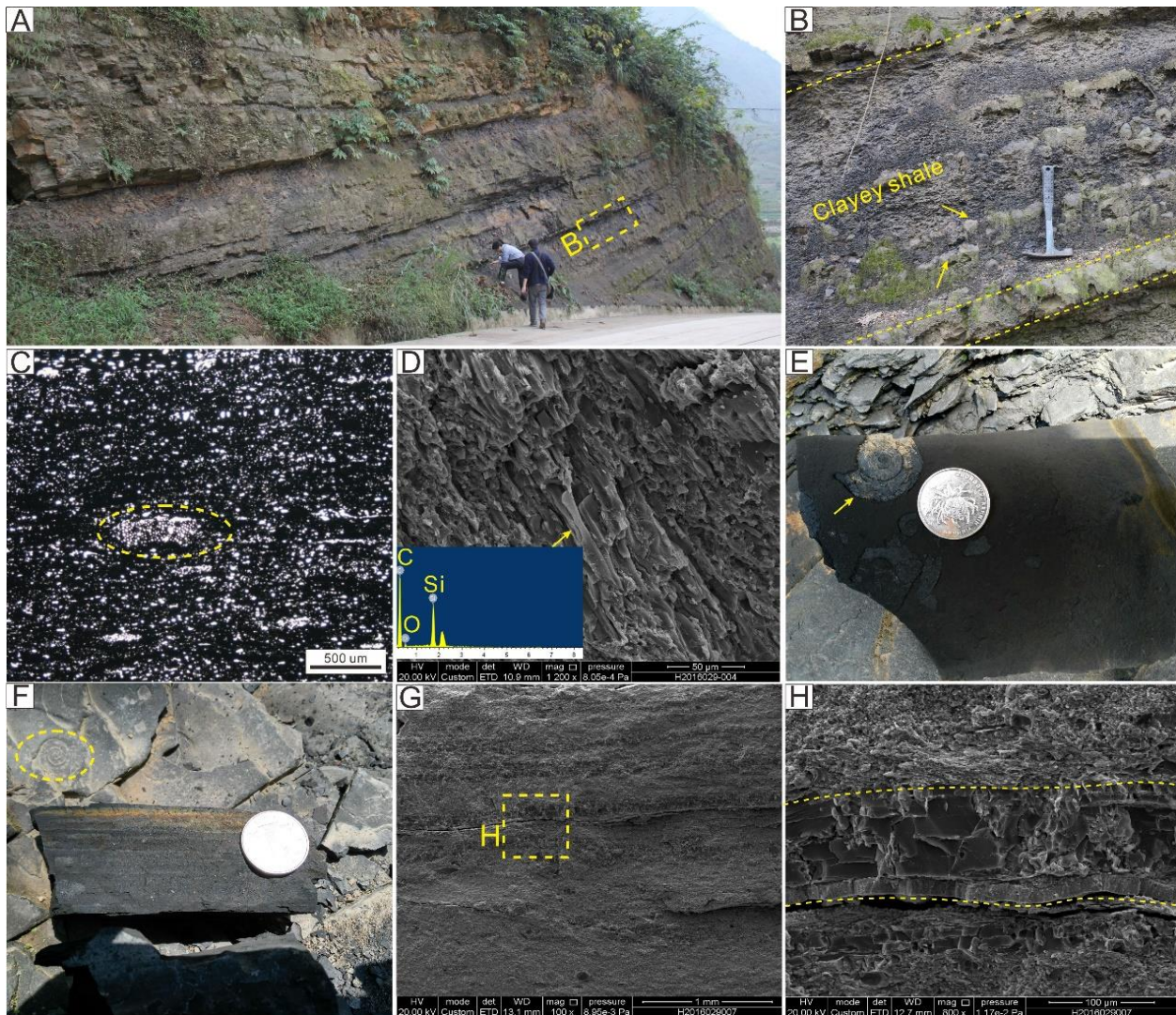


Figure 5. Characteristics of the Longtan clayey shale from field outcrops, photomicrographs and SEM images. (A) Field macroscopic characteristics of clay shale, Xinwen; (B) Clayey shale interspersed with calcareous nodules, Xinwen; (C) Plant fossil fragment in the clayey shale, PPL, Xinwen; (D) Plant fossil fragment and energy spectra, SEM, Xinqiao; (E) Ammonites up to 2 cm in length in the black clayey shale, Yuanbao; (F) Black clayey shale with horizontal laminations, Yuanbao; (G,H) organic matter and clay minerals presented in parallel, Yuanbao.

4.3.2. Carbonaceous Shale

Carbonaceous shale (CAS) is dominated by carbonate minerals, including calcite, dolomite and siderite. The XRD results show that the content of carbonate minerals ranges from 19% to 66% with an average value of 56.86%, clay minerals content ranges from 4.5% to 20.1% with an average value of 12.09%, the quartz+ pyrite+ feldspar content ranges from 11.2% to 31% with an average value of 20.42%. Some carbonaceous shale contains

certain amount of barite (Table 1), which may indicate the impact of volcanic activity [33]. Carbonaceous shale mainly deposited under tidal flats and a shallow water melanged accumulation shelf, with a lithology of mainly thin–medium layer dark gray calcareous mudstone, and foamed violently when added dilute hydrochloric acid. Carbonaceous shale interbedded with clayey shale or thin layered limestone of unequal thickness (Figure 6A,B). The deposition of CAS indicates that the carbonate factory in the basin was recovering and the terrigenous input was decreasing. Therefore, carbonaceous shale mainly developed in the middle and upper part of the Longtan Formation.

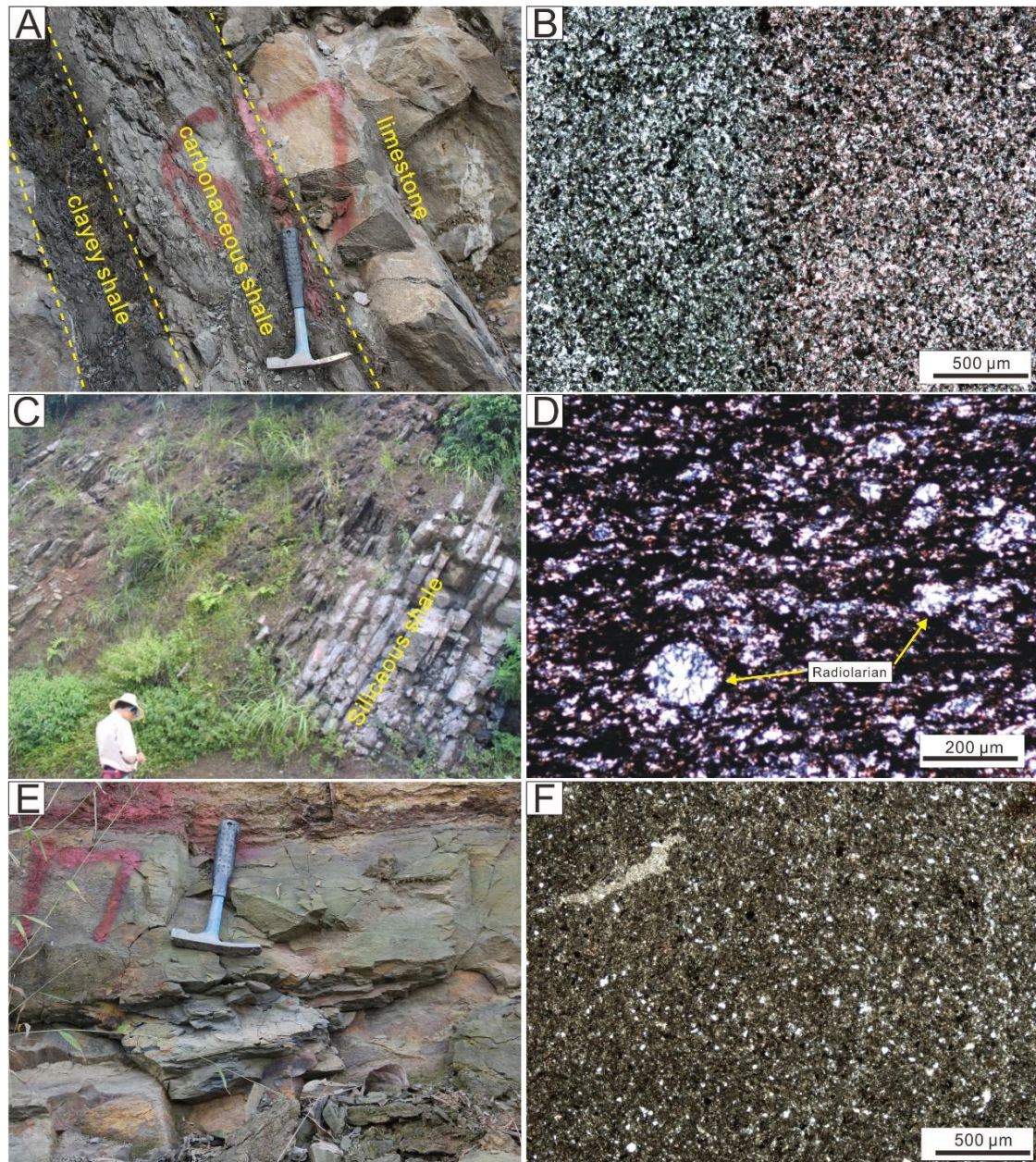


Figure 6. Characteristics of the Longtan carbonaceous shale, siliceous shale and mixed shale from field outcrops and photomicrographs. (A) Calcareous shale interbedded with clayey shale and limestone, Tianfu; (B) Microscopic characteristics of calcareous shale, stained with alizarin red, PPL, Tianfu; (C) siliceous shale interbedded with thinly layer limestone, Shizhu; (D) Silica radiolarians with black organic matter in bedded siliceous shale, Shizhu; (E) Thin to medium bedded mixed shale, Xinwen; (F) Mixed shale, lithology dominated by siltstone mudstone, PPL, Xinwen.

4.3.3. Siliceous Shale

Quartz is the main constituent minerals of siliceous shale (SS); this quartz was formed chemically or biologically, and is not detrital quartz. The content of carbonate minerals ranges from 0 to 13.1% with an average value of 3.65%, clay minerals content ranges from 1.4% to 20% with an average value of 11.04%, the quartz+ pyrite+ feldspar content ranges from 45.5% to 94% with an average value of 81.32%. Siliceous shale mainly developed in the eastern of the basin, low clay minerals content and a non-detrital quartz source indicate this type of Long shale deposited in deep water and far away from the land, such as a deep water melanged accumulation shelf. In the field outcrops, siliceous shale occurs as a thin black layer with a thickness between 5 cm and 20 cm (Figure 6C). The cryptocrystalline and microcrystalline texture of the quartz could be observed under polarizing microscope (Figure 6D); there is a small amount of carbonate minerals between the crystals and siliceous radiolaria can also be observed. The black organic matter is distributed in irregular blocks among the quartz crystals.

4.3.4. Mixed Shale

The clay minerals content ranges from 13% to 46% with an average value of 28.43%, the carbonate minerals ranges from 7% to 44.7% with an average value of 19.98%, and the quartz+pyrite+feldspar content ranges from 15.2% to 50% with an average value of 38.93%, the content of carbonate minerals ranges from 7% to 44.7% with an average value of 19.98%. The mixed shale (MS) deposited in various sedimentary environments with different mineral compositions: the shale formed in shore swamp and tidal flat environments generally has higher quartz content, and the quartz in the shale is different from that of the siliceous shale, which is mainly detrital quartz in silt grade (Figure 6E,F). The mixed shale deposited in the shallow water melanged accumulation shelf has a higher carbonate minerals content. Due to the similar sedimentary environments, mixed shale is often interbedded with calcareous shale or clayey shale.

5. Discussion

5.1. Relationships between Shale Lithofacies Assemblages and TOC

The Longtan shale has complex mineral compositions and strong heterogeneity. The TOC value of different types of Longtan Formation lithofacies shale is also quite different. The TOC value distribution histogram of the four types of Longtan shale is shown in Figure 7. The average TOC value of CLS is 5.12%, followed by SS, the average TOC value is 3.71%, the average TOC value of MS is 3.23 and the CAS has the lowest TOC value of 1.35%.

The TOC value of CLS has a large distribution range (Figure 7), from less than 0.5% to higher than 20%, which was related to the widest distribution area. CLS can be deposited in different depositional environments, and its TOC content varies greatly. The TOC of CLS deposited in shore swamp and deep water melanged accumulation shelf environments is relatively high. The TOC distribution of SS is relatively uniform (Figure 7). Although the average TOC is lower than CLS, the median is slightly higher than CLS, indicating that the TOC content of SS shale is more homogeneous than CLS. SS is the only shale lithofacies deposited in the deep-water mixed shelf environment. The TOC value of mixed shale is highly polarized. The TOC is as high as 5% to 7%, but most of them are less than 2% (Figure 7). The MS formed on the shore or on the tidal flat may contain silt-grade detrital minerals. This silty mudstone is shown as mixed shale in the Clay-carbonate-rigid particles minerals ternary diagram (Figure 3), and its TOC is low; in addition, it was formed in a shallow water melanged accumulation shelf. CAS was formed in tidal flat and shallow water mixed shelf environments. Both the average and median TOC are the lowest among the four Longtan Shales (Figure 7).

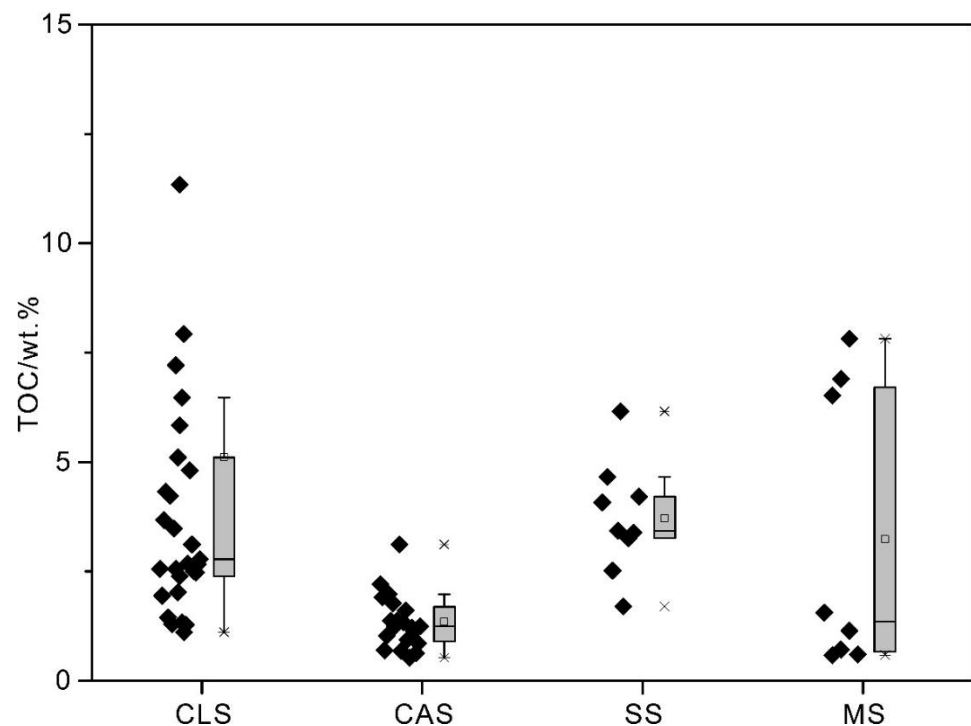


Figure 7. TOC value distribution of different Longtan shale types.

5.2. Deposition Environment Model

Sedimentary facies comparison shows the lithological, sedimentary facies characteristics and lithofacies of the Longtan Formation from southwest to northeast in the study area (Figure 8). From shore swamp and tidal flat to shallow and deep water melanged accumulation shelf, the Longtan Formation has shown a downward trend due to the influence of detrital input (Figure 9), shore swamp is most affected by terrestrial input, and carbonates were hardly developed. Therefore, CLS and MS developed in shore swamp have a high content of detrital quartz, meanwhile, a large amount of argillaceous and clay minerals deposited in the low-energy environments. The MS developed in the shore swamp is mainly argillaceous siltstone or silty mudstone, which plotted in the clay–carbonate–quartz triangle diagram as a mixture of two end members of clay minerals and quartz. The tidal flat sedimentary facies is also greatly affected by terrestrial input, but at the same time carbonate minerals and clay minerals are also relatively developed, which makes the lithology of the tidal flat facies the most complex sedimentary faices of the Longtan Formation in the study area. Except for the SS, the other three types of lithofacies were all developed in the tidal flat facies. As the water depth increases, the terrestrial input of tidal flats weakens and carbonate minerals increase. In areas closer to the land of tidal flat facies, the CAS and the MS dominated by clay minerals and carbonate minerals are mainly developed; in the area farther offshore, CAS and MS dominated by clay minerals and carbonate minerals are mainly developed.

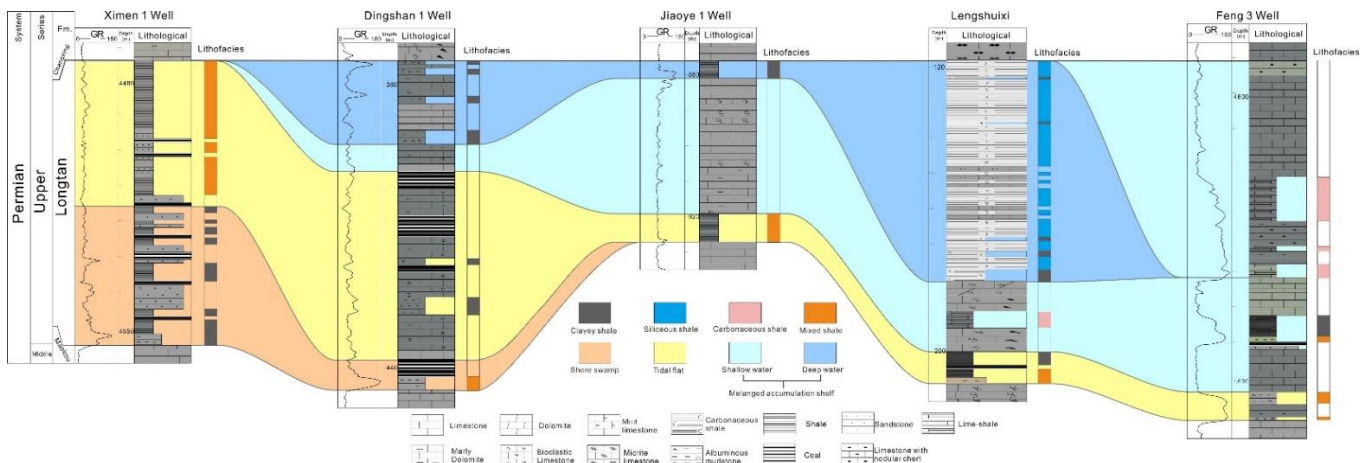


Figure 8. SW-NE cross-section through different wells in the study area.

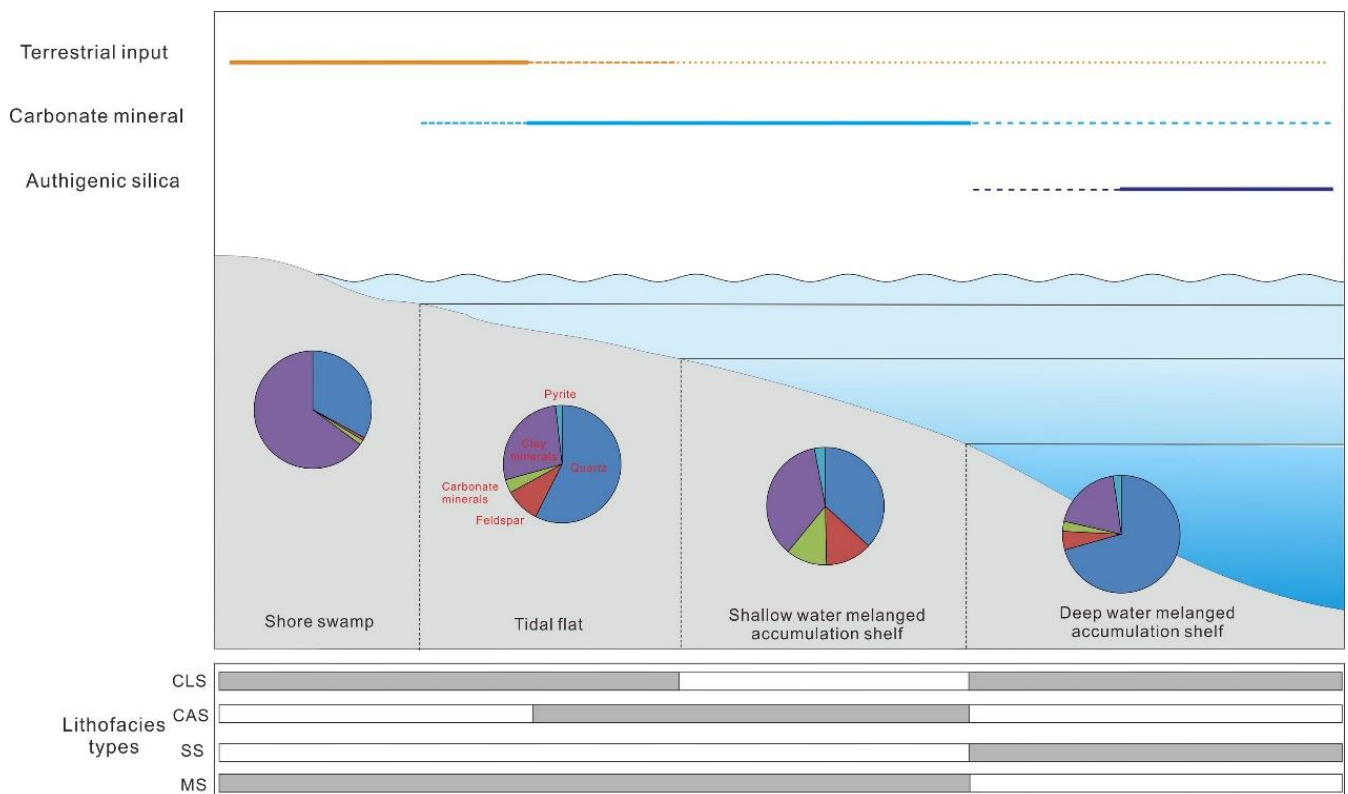


Figure 9. Depositional model of the Longtan Formation in the Sichuan Basin.

In the shallow water melanged accumulation shelf facies is less affected by terrigenous input, and the overall lithology is dominated by limestone with mudstone and shale (Figure 9). Therefore, the developed lithofacies are mainly CAS and mixed facies dominated by clay and carbonate, similar to the tidal flat sedimentary facies farther offshore. In the deep water melanged accumulation shelf facies zone, the lithofacies developed are CLS and SS. In terms of mineral composition, they are similar to shore swamp, and they are mainly composed of quartz and clay minerals. However, it is noteworthy that the quartz of deep water melanged accumulation shelf is different from the terrestrial-derived clastic quartz of shore swamp, it is a silica-rich rock formed under chemical and biological reactions in a deep water environment. Previous studies have shown that global marine chert deposition was more developed during the Permian, which is known as the Permian Chert

Event [22,34]. In the Sichuan Basin, the siliciclastic source of Permian siliciclastic rocks is multi-sourced, including biogenic, hydrothermal and terrestrial sources.

In general, the depositional environment of the Longtan Formation controls the shale mineral assemblage of the Longtan Formation and also influences the TOC content. From the present data, it seems that the shore swamp and the deep-water mixed terrigenous shelf phase zone are relatively favorable phase zones for exploration. Compared to other shale gas successfully developed worldwide, such as Barnett shale from Texas and the Longmaxi Formation shale from the Sichuan Basin (Loucks and Ruppel, 2007; Xu et al., 2019), the Longtan Formation shale has higher TOC, but also has higher clay minerals content and exhibits strong mineral heterogeneity, which requires further study.

6. Conclusions

- (1) The mineral composition of the Longtan Formation has strong mineral heterogeneity, the XRD results show that the main minerals include quartz, clay minerals, carbonate minerals (calcite, dolomite and siderite), feldspar (plagioclase and potash feldspar) and pyrite. TOC values of the Longtan Formation has a wide distribution range from 0.065% to 74.67% with an average value of 5.73% (median value of 1.59%).
- (2) Combined with thin section, SEM and XRD analysis, four types of lithofacies assemblages are distinguished: clayey mudstone, carbonaceous shale, siliceous shale and mixed shale. The TOC values of different shale lithofacies is quite different, CLS has the highest TOC content, followed by SS and MS, CAS is the lowest.
- (3) From shore swamp and tidal flat to shallow and deep water melanged accumulation shelf, the Longtan Formation has shown a downward trend due to the influence of detrital input. The shore swamp of the Longtan Formation is most influenced by the terrestrial input and mainly develops CLS and MS. The tidal flat is influenced by the terrestrial input and can also deposit carbonate minerals, developing CLS, CAS and MS. The shallow water melanged accumulation shelf develops CAS and MS dominated by clay and carbonate minerals. The deep water miscible shelf develops CLS and SS, whose mineral composition is similar to that of the shore swamp, but the quartz minerals are mainly formed by chemical and biological reactions, which are related to the Permian global chert event. The depositional environment of the Longtan Formation controls the shale mineral assemblage of the Longtan Formation and also influences the TOC content.

Author Contributions: Conceptualization, H.Y. and Y.Y.; methodology, D.L.; software, L.C. and J.H.; validation, H.Y., J.T. and W.Z.; formal analysis, Y.Y.; investigation, L.C.; resources, H.Y.; data curation, L.L.; writing—original draft preparation, H.Y.; writing—review and editing, L.L.; visualization, H.Y.; supervision, W.Z.; pro-ject administration, H.Y.; funding acquisition, L.L. All authors have read and agreed to the published version of the manuscript.

Funding: This research was funded by the National Nature Science Foundation of China [Grant 41872115].

Institutional Review Board Statement: Not applicable.

Informed Consent Statement: Not applicable.

Data Availability Statement: Not applicable.

Acknowledgments: This study was supported by the National Nature Science Foundation of China (Grant 41872115).

Conflicts of Interest: The authors declare no conflict of interest.

References

1. Zou, C.N.; Dong, D.Z.; Wang, S.J.; Li, J.Z.; Li, X.J.; Wang, Y.M. Geological characteristics and resource potential of shale gas in China. *Pet. Explor. Dev.* **2010**, *37*, 641–653. [[CrossRef](#)]
2. Liu, G.X.; Jin, Z.J.; Deng, M.; Zhai, C.B.; Guan, H.L.; Zhang, C.J. Exploration potential for shale gas in the Upper Permian Longtan Formation in southeastern Sichuan basin. *Oil Gas Geol.* **2015**, *36*, 481–487.
3. Potter, C.J. Paleozoic shale gas resources in the Sichuan Basin, China. *AAPG Bull.* **2018**, *102*, 987–1009. [[CrossRef](#)]
4. Lin, L.B.; Yu, Y.; Zhai, C.B.; Li, Y.H.; Wang, Y.N.; Liu, G.X.; Guo, Y.; Gao, J. Paleogeography and shale development characteristics of the Late Permian Longtan Formation in southeastern Sichuan Basin, China. *Mar. Petrol. Geol.* **2018**, *95*, 67–81. [[CrossRef](#)]
5. Xu, H.; Zhou, W.; Zhang, R.; Liu, S.M.; Zhou, Q.M. Characterizations of pore, mineral and petrographic properties of marine shale using multiple techniques and their implications on gas storage capability for Sichuan Longmaxi gas shale field in China. *Fuel* **2019**, *241*, 360–371. [[CrossRef](#)]
6. Zhao, J.H.; Jin, Z.J.; Hu, Q.H.; Liu, K.Y.; Liu, G.X.; Gao, B.; Liu, Z.B.; Zhang, Y.Y.; Wang, R.Y. Geological controls on the accumulation of shale gas: A case study of the early Cambrian shale in the Upper Yangtze area. *Mar. Petrol. Geol.* **2019**, *107*, 423–437. [[CrossRef](#)]
7. Hu, G.Y.; Yu, C.; Ni, Y.Y.; Huang, S.P.; Tian, X.W. Comparative study of stable carbon and hydrogen isotopes of alkane gases sourced from the Longtan and Xujiahe coal-bearing measures in the Sichuan Basin, China. *Int. J. Coal. Geol.* **2013**, *116–117*, 293–301. [[CrossRef](#)]
8. Luo, Q.Y.; Xiao, Z.H.; Dong, C.Y.; Ye, X.Z.; Li, H.J.; Zhang, Y.; Ma, Y.; Ma, L.; Xu, Y.H. The geochemical characteristics and gas potential of the Longtan formation in the eastern Sichuan Basin, China. *J. Petrol. Sci. Eng.* **2019**, *179*, 1102–1113. [[CrossRef](#)]
9. Ma, X.; Guo, S.B. Study on pore evolution and diagenesis division of a Permian Longtan transitional shale in Southwest Guizhou, China. *Energy Sci. Eng.* **2021**, *9*, 58–79. [[CrossRef](#)]
10. Zhu, Y.M.; Gu, S.X.; Li, Y.; Zou, H.Y.; Guo, T.L. Biological organic source and depositional environment of over-mature source rocks of Longtan Formation in Sichuan basin. *Geochimica* **2012**, *41*, 35–44.
11. Cao, Q.G.; Liu, G.X.; Zhang, C.J.; Pan, W.L. Sedimentary environment and its controlling on source rocks during late Permian in Sichuan Basin. *Pet. Geol. Exp.* **2013**, *35*, 36–41.
12. Wei, Z.F.; Wang, Y.L.; Wu, C.J.; Wu, B.X.; Shun, Z.P.; Li, S.X.; Wei, W. Geochemical Characteristics of Source Rock from Upper Permian Longtan Formation in Sichuan Basin. *Nat. Gas Geosci.* **2015**, *26*, 1613–1618.
13. Zhang, J.Z.; Li, X.Q.; Wei, Q.; Sun, K.X.; Zhang, G.W.; Wang, F.Y. Characterization of full-sized pore structure and fractal characteristics of marine–continental transitional Longtan Formation shale of Sichuan Basin, South China. *Energy Fuels* **2017**, *31*, 10490–10504. [[CrossRef](#)]
14. Cao, T.T.; Deng, M.; Song, Z.; Luo, H.; Hursthouse, A.S. Characteristics and controlling factors of pore structure of the Permian shale in southern Anhui province, East China. *J. Nat. Gas. Sci. Eng.* **2018**, *60*, 228–245. [[CrossRef](#)]
15. Schieber, J.; Zimmerle, W. The History and Promise of Shale Research. In *Shale and Mudstones; Basin Studies, Sedimentology and Paleontology*; Schieber, J., Zimmerle, W., Sethi, P., Eds.; Schweizerbart'sche Verlagsbuchhandlung: Stuttgart, Germany, 1998.
16. Timms, N.E.; Olierook, H.K.H.; Wilson, M.E.J.; Piane, C.D.; Hamilton, P.J.; Cope, P.; Stütenbecker, L. Sedimentary facies analysis, mineralogy and diagenesis of the Mesozoic aquifers of the central Perth Basin, Western Australia. *Mar. Petrol. Geol.* **2015**, *60*, 54–78. [[CrossRef](#)]
17. Loucks, R.G.; Ruppel, S.C. Mississippian Barnett Shale: Lithofacies and depositional setting of a deep-water shale-gas succession in the Fort Worth Basin, Texas. *AAPG Bull.* **2007**, *91*, 579–601. [[CrossRef](#)]
18. Du, X.B.; Zhang, M.Q.; Lu, Y.C.; Ping, C.; Lu, Y.B. Lithofacies and depositional characteristics of gas shales in the western area of the Lower Yangtze, China. *Geol. J.* **2015**, *50*, 683–701. [[CrossRef](#)]
19. Xiao, B.; Liu, S.G.; Ran, B.; Li, Z.W. Geochemistry and sedimentology of the Upper Ordovician-lower Silurian black shale in the northern margin of the Upper Yangtze Platform, South China: Implications for depositional controls on organic-matter accumulation. *Aust. J. Earth Sci.* **2019**, *67*, 129–150. [[CrossRef](#)]
20. Bureau of Geology and Mineral Resources of Sichuan Province (BGMRS). *Regional Geology of Sichuan Province*; Geological Publishing House: Beijing, China, 1991.
21. Wang, D.A. The geochemical feature of siliceous rocks since late proterozoic in the Yangtze platform and their genesis. *Chin. J. Geol.* **1994**, *29*, 41–54.
22. Yu, Y.; Lin, L.B.; Deng, X.L.; Wang, Y.N.; Li, Y.H.; Guo, Y. Geochemical features of the Middle–Upper Permian cherts and implications for origin, depositional environment in the Sichuan Basin, SW China. *Geol. J.* **2020**, *55*, 1493–1506. [[CrossRef](#)]
23. Cao, T.T.; Liu, G.X.; Cao, Q.G.; Deng, M. Influence of maceral composition on organic pore development in shale: A case study of transitional Longtan Formation shale in eastern Sichuan Basin. *Oil Gas Geol.* **2018**, *39*, 40–53.
24. He, J.H.; Deng, H.C.; Ma, R.L.; Wang, R.Y.; Wang, Y.Y.; Li, A. Reservoir characteristics of the Lower Jurassic lacustrine shale in the Eastern Sichuan Basin and its effect on gas properties: An integrated approach. *Energies* **2020**, *13*, 4495. [[CrossRef](#)]
25. Hao, F.; Guo, T.L.; Zhu, Y.M.; Cai, X.Y.; Zou, H.Y.; Li, P.P. Evidence for multiple stages of oil cracking and thermochemical sulfate reduction in the Puguang gas field, Sichuan basin, China. *AAPG Bull.* **2008**, *92*, 611–637. [[CrossRef](#)]
26. Ma, Y.S.; Guo, X.S.; Guo, T.L.; Huang, R.; Cai, X.Y.; Li, G.X. The Puguang gas field: New giant discovery in the mature Sichuan Basin, southwest China. *AAPG Bull.* **2007**, *91*, 627–643. [[CrossRef](#)]

27. Wang, C.S.; Li, X.H.; Chen, H.D.; Qin, J.X. Permian sea-level changes and rising-falling events in South China. *Acta Sedimentol. Sin.* **1999**, *17*, 536–541.
28. Ross, D.J.K.; Bustin, R.M. The importance of shale composition and pore structure upon gas storage potential of shale gas reservoirs. *Mar. Petrol. Geol.* **2009**, *26*, 916–927. [[CrossRef](#)]
29. Liang, Q.S.; Zhang, X.; Tian, J.C. Geological and geochemical characteristics of marine-continental transitional shale from the Lower Permian Taiyuan Formation, Taikang Uplift, southern North China Basin. *Mar. Petrol. Geol.* **2018**, *98*, 229–242. [[CrossRef](#)]
30. Curtis, J.B. Fractured shale-gas systems. *AAPG Bull.* **2002**, *86*, 1921–1938.
31. Jarvie, D.M.; Hill, R.J.; Ruble, T.E.; Pollastro, R.M. Unconventional shale-gas systems: The Mississippian Barnett Shale of north-central Texas as one model for thermogenic shale-gas assessment. *AAPG Bull.* **2007**, *91*, 475–499. [[CrossRef](#)]
32. Wang, G.C.; Carr, T.R. Methodology of organic-rich shale lithofacies identification and prediction: A case study from Marcellus Shale in the Appalachian Basin. *Comput. Geosci.* **2012**, *49*, 51–163. [[CrossRef](#)]
33. Zhang, W.Z.; Yang, H.; Xie, L.Q.; Yang, Y.H. Lake-bottom hydrothermal activities and their influence on high-quality source rock development: A case from Chang 7 source rocks in Ordos Basin. *Pet. Explor. Dev.* **2010**, *37*, 424–429.
34. Beauchamp, B.; Baud, A. Growth and demise of Permian biogenic chert along northwest Pangea: Evidence for end-Permian collapse of thermohaline circulation. *Palaeogeogr. Palaeoclimatol.* **2002**, *184*, 37–63. [[CrossRef](#)]